Time-Resolved Fluorescence Studies on the Ternary Complex Formed between Bacterial Elongation Factor Tu, Guanosine 5′-Triphosphate, and Phenylalanyl-tRNA^{Phe} †

Theodore L. Hazlett,‡ Arthur E. Johnson,§ and David M. Jameson*,‡

Department of Pharmacology, University of Texas Southwestern Medical Center, 5323 Harry Hines Boulevard, Dallas, Texas 75235, and Department of Chemistry and Biochemistry, University of Oklahoma, Norman, Oklahoma 73019

Received November 4, 1988; Revised Manuscript Received January 4, 1989

ABSTRACT: Time-resolved fluorescence spectroscopy was used to investigate the solution dynamics of *Escherichia coli* tRNA^{Phe}, Phe-tRNA^{Phe}, and Phe-tRNA^{Phe} associated with GTP and elongation factor Tu (EF-Tu) in a ternary complex. Two fluorescence probes were employed: fluorescein, covalently bound to Phe-tRNA^{Phe} at the s^4U_8 base (Phe-tRNA^{Phe}-Fl^8), and ethidium bromide, noncovalently associated with the tRNA (EB·Phe-tRNA^{Phe}). The lifetimes observed for ethidium bromide were 1.89 ns, free in solution, and 26.3 ns, bound to its tight binding site on tRNA. Fluorescein-labeled tRNA had a lifetime of 4.3 ns, with no significant difference among the values for aminoacylated, unacylated, and EF-Tu-bound Phe-tRNA^{Phe}-Fl^8. Differential phase and modulation data for each fluorophore–tRNA system were fit with local and global Debye rotational relaxation times. Local motion of the labeled fluorescein in Phe-tRNA^{Phe}-Fl^8, tRNA^{Phe}-Fl^8, and Phe-tRNA^{Phe}-Fl^8·EF-Tu·GTP was characterized by rotational relaxation times of 2.7 ± 0.5, 2.4 ± 0.4, and 2.4 ± 0.1 ns, respectively. These values are equal, within experimental error, and suggest that the rotational mobility of the s^4U_8-conjugated dye is unaffected by either tRNA^{Phe} aminoacylation or ternary complex formation. Global rotational relaxation times for Phe-tRNA^{Phe}-Fl^8, 97 ns, and EB·Phe-tRNA^{Phe}, 140 ns, were equivalent to those determined for the unacylated species, denoting little change in the overall size or shape of the tRNA molecule upon aminoacylation. These values for (Phe-)tRNA were larger than expected for a hydrated sphere of equivalent volume, 83 ns, and therefore confirm the asymmetric nature of the tRNA structure in solution. In the presence of EF-Tu the global rotational relaxation times increased to 175 ns (fluorescein) and to 223 ns (ethidium bromide). The ratio of the observed rotational relaxation time to that predicted for a hydrated sphere of equivalent volume (163 ns for the ternary complex) is less for the ternary complex than for either Phe-tRNA^{Phe}-Fl^8 or EF-Tu by itself. This result indicates that the ternary complex is more symmetrical than either macromolecular subunit, which suggests that the molecular arrangement of the asymmetric components in this complex is more side by side than end to end.

Prokaryotic protein biosynthesis requires the formation of a ternary complex consisting of aminoacyl-tRNA (aa-tRNA),[1] GTP, and a nonribosomal protein designated elongation factor Tu (EF-Tu) (Miller & Weissbach, 1977a,b). This complex initiates each elongation cycle by binding to the ribosome and beginning the aa-tRNA recognition process. When the aa-tRNA anticodon is complementary to the mRNA codon, the aa-tRNA binding process is completed by the hydrolysis of the GTP, the release of the resulting EF-Tu·GDP from the ribosome, and the movement of the aa-tRNA into the A site on the ribosome.

In order to elucidate the molecular mechanisms that control aa-tRNA recognition and binding at the ribosome, and therefore translational accuracy, we must understand the energetic, structural, and dynamic aspects of the ternary complex. Crystallography has provided structures for the individual macromolecules in the ternary complex, i.e., elongator tRNAs (Kim & Rich, 1968; Ladner et al., 1972; Kim et al., 1974; Sigler, 1975) and a trypsin-modified EF-Tu·GDP (Morikawa et al., 1978; Jurnak, 1985; LaCour et al., 1985). However, similar diffraction data on the ternary complex have not been forthcoming, and the relative orientation of the aa-tRNA and the EF-Tu in this ternary complex is still unknown.

The dynamic behavior of the tRNA molecule has been investigated both in solution and in the crystal lattice [reviewed by Rigler and Wintermeyer (1983)]. Analysis of the temperature factors and mean square displacement of each atom from the average atomic position has been carried out for crystals of yeast tRNA^{Phe} (Sussman et al., 1978; Holbrook et al., 1978). The largest temperature factors were found in the anticodon loop and the acceptor end. ^{13}C NMR studies on selectively modified base methyl groups of yeast tRNA, however, indicated that the nucleotides with the most restricted internal motions are in the anticodon loop (Schmidt et al., 1987). The conformational dynamics of the anticodon loop in solution were also investigated by using time-resolved anisotropy studies of wybutine (Claesens & Rigler, 1986). The

† This work was supported by Grants DMB-8706440 from the National Science Foundation (D.M.J.) and GM26494 from the National Institutes of Health (A.E.J.). D.M.J. is an Established Investigator of the American Heart Association. A preliminary report of this work has been presented at the Jan 1988 meeting of The Society of Photo-Optical Instrumentation Engineers.

* To whom correspondence should be addressed.

‡ University of Texas Southwestern Medical Center.

§ University of Oklahoma.

[1] Abbreviations: EF-Tu, elongation factor Tu; aa-tRNA, aminoacyl-tRNA; s^4U, 4-thiouridine; tRNA^{Phe}-Fl^8, adduct between 5-(iodoacetamido)fluorescein and the s^4U_8 base of tRNA^{Phe}; EB, 2,7-diamino-9-phenyl-10-ethylphenanthridinium bromide (ethidium bromide); GTP, guanosine 5′-triphosphate; GDP, guanosine 5′-diphosphate; Tris, tris(hydroxymethyl)aminomethane; PK, pyruvate kinase; PMSF, phenylmethanesulfonyl fluoride; PEP, phosphoenolpyruvate; DTT, dithiothreitol; HEPES, *N*-(2-hydroxyethyl)piperazine-*N*′-2-ethanesulfonic acid.

0006-2960/89/0428-4109$01.50/0

results suggested that, in the presence of Mg^{2+}, wybutine was immobile, yet its rotational mobility increased significantly upon association with the complementary codon. Similar studies on the dynamic aspects of the macromolecular components in the ternary complex, either in solution or in crystals, have not appeared.

Some specific structural information on the ternary complex is available from a variety of biochemical and chemical studies. Nuclease digestion, chemical modification, and hydrolysis protection studies indicate that the protein binds to the aminoacyl end of the aa-tRNA and along the amino acid acceptor and TΨC helices, while the anticodon loop and stem are exposed in the ternary complex [for references, see Miller and Weissbach (1977b) and Johnson et al. (1986)]. In addition, the region near the s^4U_8 base at the inside corner of the tRNA "L" is accessible to solvent in the ternary complex (Adkins et al., 1983), and the D loop also appears to be exposed (Jekowsky et al., 1977). Affinity labeling experiments have identified contact sites between the macromolecules: His-66 of EF-Tu reacts covalently and with high efficiency with the amino acid side chain of a modified Lys-tRNA (Johnson et al., 1978; Duffy et al., 1981), and Lys-208 and Lys-237 can be cross-linked to the 3′-terminal ribose of unacylated tRNA (van Noort et al., 1984). The absence of an identified contact site elsewhere in the ternary complex, however, limits our understanding of the relative orientation of the macromolecules and hence the overall size and structure of this protein–nucleic acid complex.

Solution studies on the ternary complex employing small-angle X-ray scattering (Österberg et al., 1981) and small-angle neutron scattering (Antonsson et al., 1986) have been reported, but their conclusions appear to differ substantially. The former study suggests that the valyl-$tRNA^{Val}$·EF-Tu·GTP complex has a radius of gyration of 36 Å and that the maximum distance within the complex is 125 Å. From this model the authors conclude that the anticodon stem and loop protrude into the solution. In contrast, the small-angle neutron scattering study on the same system indicated that the complex had a radius of gyration equal to 25.7 Å with a distance between the tRNA and protein centers of mass of 28 Å. Moreover, this latter study suggested that the complex was compact rather than extended.

In order to provide new information about structural and dynamic aspects of the ternary complex, as well as to address the differences noted above, we have examined the ternary complex using time-resolved fluorescence methods. These methods primarily yield hydrodynamic information about appropriately labeled macromolecular complexes, but a particular advantage of the time-resolved approach is its ability to readily distinguish between fast, local motions of the probe and the slower, global motion of the macromolecule. Specifically, we have used two extrinsic fluorophores, one attached covalently to the aa-tRNA and the other bound noncovalently to a specific site on the aa-tRNA, to monitor the environments and rotational modalities (local and global) of two distinct sites in free aa-tRNA and, more importantly, in the ternary complex. The results not only provide information about the structure and dynamics of the ternary complex but also demonstrate the utility of this approach in analyzing protein–nucleic acid interactions.

Materials and Methods

Chemicals and Reagents. Guanosine 5′-diphosphate (GDP), ribonuclease A, guanosine 5′-triphosphate (GTP), tris(hydroxymethyl)aminomethane (Tris), rabbit muscle pyruvate kinase (PK), phenylmethanesulfonyl fluoride (PMSF), phosphoenolpyruvate (PEP), NaN_3, and ethidium bromide were purchased from Sigma Biochemicals. [8-^{3}H]GDP was from Amersham. Dithiothreitol (DTT) was purchased from Pierce Chemical Co. and *N*-(2-hydroxyethyl)piperazine-*N*′-2-ethanesulfonic acid (HEPES) from United States Biochemical Corp.

Elongation Factor Tu. Elongation factor Tu was purified from *Escherichia coli* MRE 600 paste (Grain Processing, Inc.) as described elsewhere (Leberman et al., 1980) or was obtained as a kind gift from Dr. John Eccleston (MRC Laboratories, Mill Hill, London) or Dr. Frances Jurnak (University of California at Riverside, Riverside, CA). EF-Tu·GDP was stored in 50 mM Tris (pH 7.6), 10 mM $MgCl_2$, 0.5 mM DTT, 1 mM NaN_3, and 0.01 mM PMSF at −80 °C. The concentration of active EF-Tu was routinely determined by using the GDP-binding assay described in the literature (Miller & Weissbach, 1974). The extinction coefficient of EF-Tu·GDP at 280 nm was found to be 29 200 M^{-1} cm^{-1} by quantitative amino acid analysis, and this value was utilized to determine the total concentration of EF-Tu. This extinction coefficient is close to the theoretical value of 26 600 M^{-1} cm^{-1}, which was determined by summing the molar extinction coefficients of the absorbing species present in EF-Tu (Edelhoch, 1967) and using a molar extinction coefficient for GDP at 280 nm of 7800 M^{-1} cm^{-1} (Bock et al., 1956). When EF-Tu was unfolded in 6 M guanidine hydrochloride, less than a 1% change in the absorption at 280 nm was observed. Hence, none of the absorbing residues [3 cysteines, 1 tryptophan, 10 tyrosines, and 1 GDP (Arai et al., 1980; Laursen et al., 1981)] were in environments that significantly altered their molar extinction coefficients from the values observed in nondenaturing conditions. This newly determined extinction coefficient for EF-Tu·GDP is substantially closer to the theoretical value than the extinction coefficients previously reported (Arai et al., 1973; Miller & Weissbach, 1977a).

tRNA. Pure *E. coli* $tRNA^{Phe}$ was purchased from Subriden RNA (Rolling Bay, WA), while unfractionated yeast tRNA and yeast $tRNA^{Phe}$ (95% $tRNA^{Phe}$) were purchased from Sigma Biochemicals. *E. coli* $tRNA^{Phe}$-Fl^8, with the fluorescein moiety covalently attached to the s^4U at position 8, was prepared and purified as described previously (Johnson et al., 1982). Aminoacylation of the $tRNA^{Phe}$ and $tRNA^{Phe}$-Fl^8 was accomplished and quantified as detailed elsewhere (Johnson et al., 1982; Abrahamson et al., 1985). The extents of aminoacylation of the samples used in this study were 1333 pmol of Phe/A_{260} unit for Phe-$tRNA^{Phe}$-Fl^8 (83% aminoacylated) and either 1320 or 990 pmol of Phe/A_{260} unit for Phe-$tRNA^{Phe}$ (83% and 62% aminoacylated, respectively). Transfer RNA concentrations were determined by using $\epsilon_{260} = 6.25 \times 10^5$ M^{-1} cm^{-1} (Adkins et al., 1983). In the experiments with ethidium the tRNA concentration was 1.8 or 20 μM; the probe concentration in these cases was 3.9 μM. The concentration of fluorescein-labeled tRNA in the reported experiments was 0.21 μM unless otherwise stated. The extent of deacylation of [^{14}C]Phe-$tRNA^{Phe}$(-Fl^8) during an experiment was measured by separating tRNA-associated radioactivity from free [^{14}C]phenylalanine on a G-25 desalting column (Abrahamson et al., 1985). Average deacylation of Phe-$tRNA^{Phe}$(-Fl^8) during experiments with the ternary complex was 4%.

Sample Preparation. Samples routinely contained buffer A [50 mM HEPES (pH 7.6), 10 mM $MgCl_2$, and 50 mM NH_4Cl], unless stated otherwise, and measurements were carried out at 5 °C to reduce the amount of Phe-$tRNA^{Phe}$(-Fl^8) deacylation during the experiments. Samples in which the ternary complex was to be formed also contained 1.5 mM PEP,

25 μM GTP, and 50 μg/mL PK.

EF-Tu·GTP was prepared by incubating EF-Tu·GDP for 30 min at 37 °C in the presence of 1.5 mM PEP, 25 μM GTP, and 50 μg/mL PK; the EF-Tu·GTP was maintained in ice until needed. Addition of EF-Tu·GTP [routinely at a 3- and 4-fold molar excess over the sample Phe-tRNA^{Phe}(-Fl^{8}) concentration] to an aa-tRNA-containing sample was followed by incubation at 37 °C for 2 min before cooling to 5 °C. Fluorescence measurements on free Phe-tRNA^{Phe}·EB or Phe-tRNA^{Phe}-Fl^{8} were carried out either before EF-Tu·GTP addition or after the release of aa-tRNA from the ternary complex by the addition of excess GDP (5 mM). The presence or absence of PEP, PK, and GTP did not interfere with the lifetime or differential phase data in either the fluorescein-labeled tRNA system or the ethidium bromide system. Ethidium bromide and GDP (=GTP) concentrations were determined by using ϵ_{480} = 5300 M^{-1} cm^{-1} (Hudson & Jacobs, 1975) and ϵ_{253} = 13 700 M^{-1} cm^{-1} (Bock et al., 1956), respectively.

Time-Resolved Measurements. Lifetime and dynamic polarization measurements were carried out by using a home-built multifrequency and phase modulation fluorometer based on the Gratton design (Gratton & Limkeman, 1983). Excitation of ethidium bromide was accomplished by using the 514.5-nm line of an argon ion laser (Spectra Physics Model 2025), and emission at wavelengths greater than 555 nm was observed through Schott OG 550 and OG 570 cut-on filters. Fluorescein and fluorescein-labeled tRNA were excited with the 488-nm argon ion laser line, and emission at wavelengths greater than 515 nm was observed through Schott OG 515 and OG 530 cut-on filters.

In the multifrequency phase and modulation technique, the intensity of the exciting light is modulated and the phase shift and relative modulation of the emitted light are determined with respect to the excitation or known lifetime standard. In the present study, dilute solutions of glycogen were used for the scattering signal; fluorescein in 0.1 M NaOH (τ = 4.05 ns) and ethidium bromide in buffer A at 5 °C (τ = 1.89 ns) also were used as references for the Phe-tRNA^{Phe}-Fl^{8} and ethidium–tRNA systems, respectively, to verify that "color effects" did not have a detectable influence in our instrument (Jameson et al., 1984). Phase and modulation lifetimes (τ^{P} and τ^{M}) were then calculated according to the equations:

$$\tan [P] = \omega\tau^{P} \quad (1)$$

$$M = [1 + (\omega\tau^{M})^2]^{-1/2} \quad (2)$$

where P is the phase shift, M the relative modulation, and ω the angular modulation frequency (Gratton et al., 1984). An emitting system characterized by a single-exponential decay will yield identical phase and modulation lifetimes irrespective of the modulation frequency. In the case of heterogeneous emitting systems (multiple noninteracting fluorescent species), the phase lifetime will be less than the modulation lifetime. Furthermore, both of these apparent lifetimes will then depend upon the modulation frequency, namely, decreasing as the modulation frequency increases (Gratton et al., 1984). The measured phase and modulation values may be analyzed by assuming either a sum of exponentials or by a new and alternative approach that involves the use of continuous lifetime distribution models (Alcala et al., 1987). In both cases the goodness of the fit may be judged by the value of the reduced χ^2 (Jameson et al., 1984), defined as

$$\chi^2 = \sum\{[(P_c - P_m)/\sigma^{P}]^2 + [(M_c - M_m)/\sigma^{M}]^2\}/(2n - f - 1) \quad (3)$$

The sum is carried over the measured values at n modulation frequencies, and f is the number of free parameters. The symbols P and M correspond to phase shift and relative modulation values, respectively, while the indices c and m indicate the calculated and measured values. σ^{P} and σ^{M} are the standard deviations of each phase and modulation measurement, respectively. Analyses were performed by using a constant, frequency-independent standard deviation of 0.2° for σ^{P} and 0.004 for σ^{M}. The calculated values of phase and modulation were obtained by using the equations:

$$P = \tan^{-1} [S(\omega)/G(\omega)] \quad (4)$$

$$M^2 = S(\omega)^2 + G(\omega)^2 \quad (5)$$

$S(\omega)$ and $G(\omega)$ have different expressions depending on the fitted model utilized. For the fit using the sum of exponentials, the functions $S(\omega)$ and $G(\omega)$ are given by

$$S(\omega) = \sum\{f_i\omega\tau_i/(1 + \omega^2\tau_i^2)\} \quad (6)$$

$$G(\omega) = \sum\{f_i/(1 + \omega^2\tau_i^2)\} \quad (7)$$

$$\sum f_i = 1 \quad (8)$$

where the index i depends upon the number of exponentials used for the fit, τ_i is the lifetime of the ith component, and f_i is the contribution of the ith component to the total intensity.

In the dynamic polarization measurements, the sample is illuminated by light polarized parallel to the vertical laboratory axis with intensity modulated at variable frequencies. The phase delay $\Delta\Phi$ between the perpendicular and parallel components of the emission can then be directly determined as well as the ratio of their ac components, Y. For an isotropic rotation one obtains the expressions (Weber, 1977):

$$\Delta\Phi = \tan^{-1} \{(18\omega r_0 R)/[[(k^2 + \omega^2) \times (1 + r_0 - 2r_0^2)] + 6R(6R + 2k + kr_0)]\} \quad (9)$$

$$Y^2 = \{[(1 - r_0)k + 6R]^2 + (1 - r_0)^2\omega^2\}/\{[(1 + 2r_0)k + 6R]^2 + (1 + 2r_0)^2\omega^2\} \quad (10)$$

where r_0 is the limiting anisotropy, R the rotational diffusion coefficient, and k the radiative rate constant ($1/\tau$).

For a fluorophore associated with a macromolecule, the expression for the differential phase and modulation may contain more terms. A macromolecule is generally not an isotropic rotator, and rotational relaxation times about the various axes will affect the results. Also, the observed rotational relaxation times will depend upon the orientation of the fluorophore's absorption and emission dipoles with respect to these macromolecular axes (Beechem et al., 1986). In the present analysis of the fluorescein–tRNA system, we are interested in distinguishing local mobility of the probe from the global rotational rate of the macromolecular species. The precise equations used to model such systems will clearly depend upon the complexities of the specific case, such as whether or not the local motion is anisotropic or hindered, and the orientation of the emission dipole of the probe with respect to the relevant molecular axes. In the absence of more detailed structural information we have adopted the simplest, limiting case (Jameson et al., 1987), i.e.

$$r(t) = r_0(g_1 e^{-\tau/\Theta_1} + g_2 e^{-\tau/\Theta_2}) \quad (11)$$

where r_0 is the time zero anisotropy (the limiting anisotropy), τ is the fluorescence lifetime, Θ_1 and Θ_2 are the rotational correlation times (equal to the Debye rotational relaxation time divided by 3) associated with the global and local rotations, respectively, and g_1 and g_2 are the associated amplitude (preexponential) factors. The equation was converted to the

Table I: Lifetime Parameters[a]

species[b]	τ_1 (ns)	f_1	τ_2 (ns)	f_2	τ_3 (ns)	f_3	$\langle\chi^2\rangle$
fluorescein (4)	4.05 ± 0.02	1.00					2.0
tRNA^{Phe}-Fl^8 (5)							
one component	4.00 ± 0.11	1.00					42.3
two component (fixed scatterer)	4.27 ± 0.04	0.97 ± 0.01	0.001[c]				3.6
Phe-tRNA^{Phe}-Fl^8 (6)	4.29 ± 0.02	0.99 ± 0.02	0.001[c]				1.9
Phe-tRNA^{Phe}-Fl^8·EF-Tu·GTP (5)	4.31 ± 0.03	0.98 ± 0.02	0.001[c]				0.9
ethidium bromide (EB) (5)	1.89 ± 0.02	1.00					1.9
EB·tRNA ([tRNA] ≫ [EB]) (4)[d]	26.3 ± 0.20	0.99 ± 0.01	1.9[c]				1.3
EB·Phe-tRNA^{Phe} (4)	26[c]	0.51 ± 0.05	12.3 ± 3.8	0.31 ± 0.09	1.9[c]	0.18 ± 0.05	1.4
EB·Phe-tRNA^{Phe}·EF-Tu·GTP (4)	26[c]	0.45 ± 0.04	14.3 ± 1.2	0.33 ± 0.04	1.9[c]	0.22 ± 0.05	3.0

[a] Fractional intensities (f), $\langle\chi^2\rangle$ values, and fluorescence lifetimes (τ) were determined as described under Materials and Methods in buffer A at 5 °C (except for free fluorescein, which was in 0.1 M NaOH). [b] Average over (n) samples ± the standard deviation. [c] A lifetime value was fixed for a scatterer (0.001 ns), free ethidium bromide (1.9 ns), and the tight ethidium bromide binding site (26 ns) where indicated. Their respective fractional weights were treated as variables in the analysis routines. [d] tRNA used here was yeast tRNA^{Phe} at concentrations where the tight binding site was the primary site bound (4 μM ethidium bromide and 20 μM tRNA).

frequency domain by using the method outlined by Weber (1977), and then a fit was performed by using a nonlinear least-squares analysis with software from ISS, Inc. (Champaign, IL). As with the lifetimes analyses, frequency-independent standard deviations of 0.2° for phase and 0.004 for modulation were used in the χ^2 routines.

Debye rotational relaxation times for hydrated spheres that have the same volume as either tRNA or the ternary complex were calculated according to the equation:

$$\rho = 3(V + \delta)\eta/\kappa T \qquad (12)$$

where V is the molecular volume, δ the partial specific volume associated with the water of hydration, η the viscosity, κ the Boltzmann constant, and T the absolute temperature. The molecular volume for EF-Tu·GTP was calculated by using a molecular weight of 43 200 (Arai et al., 1980) and a specific volume of 0.74 mL/g [determined from the sequence (Arai et al., 1980; Laursen et al., 1981) by summing the volume of the constituent amino acids (Cohn & Edsall, 1943; McMeekin et al., 1949)]. The molecular volume for *E. coli* tRNA^{Phe} was determined from the specific volume, 0.503 mL/g (Tao et al., 1970), and a molecular weight of 25 000 (Barrell & Sanger, 1969; Uziel & Gassen, 1969). The hydrations used for tRNA and EF-Tu·GTP were 1.2 mL/g (Tao et al., 1970) and 0.2 mL/g, respectively. The volume of the hydrated ternary complex was assumed to be equal to the sum of the volumes of its hydrated subunits, aa-tRNA and EF-Tu·GTP. The ratio of the observed rotational relaxation time to that of a sphere of equal volume is related to the shape and size of the rotating species. In turn, this ratio of rotational relaxation times can be related to the axial ratios of a hydrodynamically equivalent ellipsoid of revolution (Tao et al., 1970).

Results

Lifetimes. Phase and modulation data points and the theoretical curve for a representative sample of Phe-tRNA^{Phe}-Fl^8 are shown in Figure 1. Multiple samples of fluorescein, tRNA^{Phe}-Fl^8, Phe-tRNA^{Phe}-Fl^8, and Phe-tRNA^{Phe}-Fl^8·EF-Tu·GTP were analyzed, and the average lifetime values are reported in Table I. Fluorescein in 0.1 M NaOH was well fit to a single lifetime of 4.05 ns. Analyses of 5 data sets on unacylated tRNA^{Phe}-Fl^8 showed that a two-component model with the second component fixed to 0.001 ns gave significantly better fits than did single-lifetime analyses. The short component constitutes a correction for scattered light (Rayleigh or water Raman) not removed by the cut-on filters. Lifetimes were found to be 4.3 ns for unacylated tRNA^{Phe}-Fl^8, Phe-tRNA^{Phe}-Fl^8, and Phe-tRNA^{Phe}-Fl^8·EF-Tu·GTP. Additionally, Phe-tRNA^{Phe}-Fl^8 digested with RNase A gave a lifetime of 4.09 ns, close to the value for fluorescein in alkaline solution. Saturating concentrations of EF-Tu·GTP were used to ensure complete binding of the Phe-tRNA^{Phe}-Fl^8 to the protein (Abrahamson et al., 1985). In several cases, complex formation was also followed by monitoring the increase in fluorescence intensity that accompanies ternary complex formation (Adkins et al., 1983).

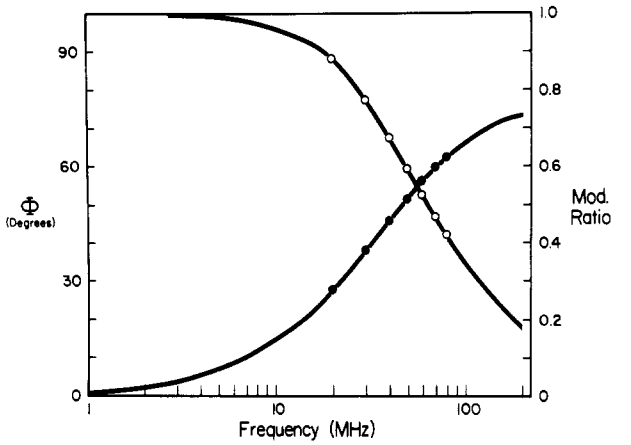

FIGURE 1: Lifetime multifrequency phase (●) and modulation (○) data for Phe-tRNA^{Phe}-Fl^8 (0.2 μM) at 5 ° C excited at 488 nm; emission measured through Schott OG 515 and OG 530 cut-on filters that passed wavelengths greater than 515 nm. Sample also contained 0.6 μM EF-Tu·GDP (therefore no ternary complex). Curves represent the least-squares best fit to the data points.

At 5 °C ethidium bromide has a single short lifetime, 1.89 ns, which increases to 26.3 ns in the presence of an excess of tRNA. These values compare well to those reported by others (Tao et al., 1970; Jones et al., 1978; Thomas et al., 1984; Ferguson & Yang, 1986). Data and the best-fit curves to free and tRNA-bound ethidium bromide are shown in Figure 2. Averages and standard deviations of multiple samples are given in Table I. When tRNA was in excess, and essentially all ethidium bromide was bound to the single tight binding site, a single (99% fractional intensity) lifetime component was resolved. Though not extensively examined, this lifetime did not appear to change significantly with temperature. The lifetime of free ethidium bromide, on the other hand, decreases slightly to 1.78 ns at 20 °C (data not shown).

When the tRNA/ethidium bromide ratio was decreased, additional lifetime components were apparent (Figure 2 and Table I) which presumably result from ethidium binding to secondary sites on the tRNA (Bittman, 1969; Wells & Cantor, 1977; Jones et al., 1978). Further experiments to elucidate the number and nature of the additional sites were beyond the

Table II: Dynamic Polarization Parameters[a]

species[b]	ρ_1 (ns)	r_1	ρ_2 (ns)	r_2	$\langle\chi^2\rangle$
fluorescein (4)	0.66 ± 0.06	0.380[c]			3.48
$tRNA^{Phe}$-Fl^8 (4)					
one component	47 ± 3	0.313 ± 0.012			16.44
two component	95 ± 10	0.271 ± 0.015	2.7 ± 0.5	0.081 ± 0.007	0.32
Phe-$tRNA^{Phe}$-Fl^8 (6)	97 ± 5	0.266 ± 0.016	2.4 ± 0.4	0.092 ± 0.009	0.33
Phe-$tRNA^{Phe}$-Fl^8·EF-Tu·GTP (3)	175 ± 13	0.263 ± 0.017	2.4 ± 0.1	0.091 ± 0.002	0.22
ethidium bromide (EB) (3)	0.54 ± 0.03	0.360[c]			2.05
EB·$tRNA^{Phe}$([tRNA] ≫[EB]) (3)[b]	142 ± 1	0.344 ± 0.019	11 ± 2	0.029 ± 0.004	1.01
EB·Phe-$tRNA^{Phe}$ (3)	140 ± 5	0.258 ± 0.013	12 ± 3	0.076 ± 0.002	0.31
EB·Phe-$tRNA^{Phe}$·EF-Tu·GTP (3)	223 ± 6	0.242 ± 0.023	16 ± 6	0.086 ± 0.020	0.41
theoretical (spherical) values[d]					
Phe-$tRNA^{Phe}$	83				
Phe-$tRNA^{Phe}$·EF-Tu·GTP	163				

[a] Debye rotational relaxation times (ρ), $\langle\chi^2\rangle$ values, and anisotropy amplitudes (r) were determined as described under Materials and Methods in buffer A at 5 °C (except fluorescein; see Table I) and were fit aided by the lifetime values and fractional intensities reported in Table I. Data reported above have been corrected for heterogeneity (see text) and describe the noted species only. Analyses of the data included, where appropriate, values for the presence of unbound $tRNA^{Phe}$(-Fl^8) and free ethidium bromide. [b] As in Table I. [c] Determined for free dye in 98% glycerol at 0 °C and fixed in the analysis procedures. [d] Values of ρ_1 calculated at 5 °C for a sphere of the same volume as the hydrated species shown.

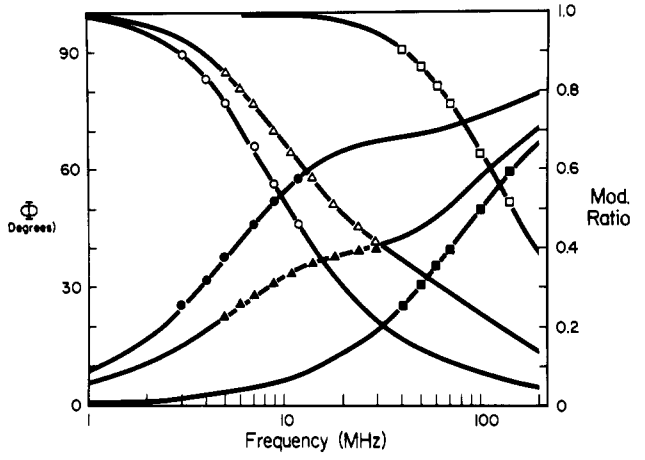

FIGURE 2: Lifetime multifrequency phase (closed symbols) and modulation (open symbols) data for ethidium bromide (20 μM) (■, □), ethidium bromide (3.9 μM) in the presence of yeast tRNA (20 μM) (●, ○), and ethidium bromide (3.9 μM) in the presence of *E. coli* Phe-$tRNA^{Phe}$ (1.8 μM) (▲, △). Measurements were performed at 5 °C and excited at 514.5 nm; emission was observed at wavelengths greater than 555 nm through Schott OG 550 and OG 570 cut-on filters. Curves represent best-fit analyses to the data points.

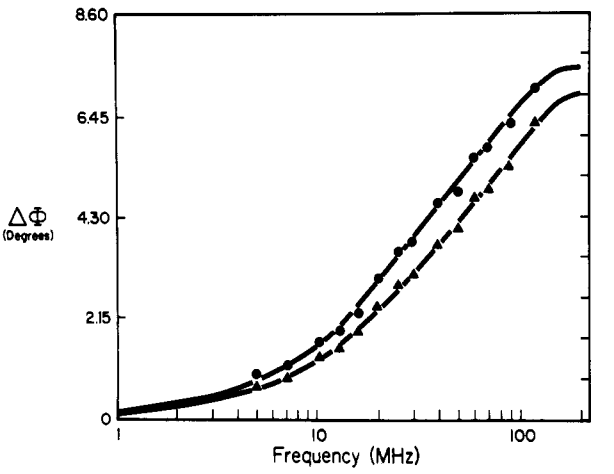

FIGURE 3: Differential phase data for Phe-$tRNA^{Phe}$-Fl^8 (0.25 μM) in the presence (▲) and absence (●) of EF-Tu·GTP (3 μM). Data were taken at 5 °C with an excitation at 488 nm; emission was observed at wavelengths above 515 nm through Schott OG 515 and OG 530 filters. Curves represent best-fit analyses to both phase and modulation (not shown) data points.

scope of this study and were not pursued. The known lifetimes of free probe (1.9 ns) and of probe in the tight binding site (26 ns) were routinely fixed in the analyses.

Rotational Analyses. Dynamic polarization measurements were carried out on samples of $tRNA^{Phe}$-Fl^8 and Phe-$tRNA^{Phe}$-Fl^8 (Figure 3 and Table II). In all cases, fitting to a single rotational relaxation time gave poor agreement between data points and predicted curve. Also, single-component analysis of the unacylated $tRNA^{Phe}$-Fl^8 data resulted in a single rotational relaxation time of 47 ns, significantly shorter than the values (90–145 ns; adjusted for 5 °C) reported for tRNA in the literature (Tao et al., 1970; Thomas et al., 1984; Ferguson & Yang, 1986) or the theoretical rotational relaxation time for a sphere of volume equal to the tRNA's (Table II). In contrast, the two-component fit gave a slow rotational relaxation time of 95 ns, consistent with the value expected for the overall motion of tRNA, and a fast rotational relaxation time of 2.7 ns, due most likely to a fast structural motion at the probe's point of attachment. We do not ascribe this fast rotational component to free fluorescein since (i) gel filtration chromatography before and after the fluorescence measurements did not indicate the presence of free fluorescein and (ii) the rotational and lifetime properties of free fluorescein were not consistent with those observed for the fast component of (Phe-)$tRNA^{Phe}$-Fl^8. No significant differences between the rotational parameters of $tRNA^{Phe}$-Fl^8 and Phe-$tRNA^{Phe}$-Fl^8 were found.

In the presence of EF-Tu·GTP, a slight drop in the modulation ratio and a more significant change in the phase difference was observed with Phe-$tRNA^{Phe}$-Fl^8 (Figure 3). Rotational analyses showed that ternary complex formation resulted in a large increase in the slower, global rotational relaxation time, as would be expected due to the increased size of the complex, but that no change in the fast (2.4-ns) component was evident (Table II). The fractional amount of unacylated $tRNA^{Phe}$-Fl^8, which does not bind to EF-Tu in the sample, was fixed in the analysis as a second component. The presence of significant amounts of free Phe-$tRNA^{Phe}$-Fl^8 in these samples is unlikely since the concentrations of EF-Tu·GTP (≥0.75 μM) and of aa-tRNA (≈0.25 μM) were both considerably larger than the 1 nM dissociation constant of the ternary complex in this solvent (Abrahamson et al., 1985).

The concentration of $tRNA^{Phe}$-Fl^8 in a sample was determined from the initial specific activity of the Phe-$tRNA^{Phe}$-Fl^8 and the amount of aminoacyl bond hydrolysis during the experiment. Since the rotational relaxation times determined for acylated and unacylated samples were nearly identical (Table II), the rotational parameters used for $tRNA^{Phe}$-Fl^8 in the analysis of the ternary complexes were those determined

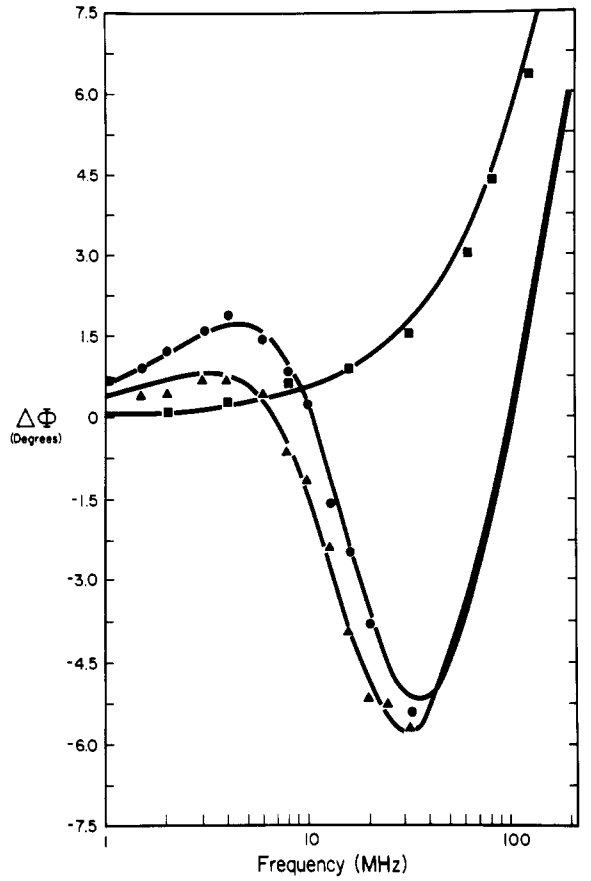

FIGURE 4: Differential phase data taken at 5 °C for ethidium bromide (20 μM) (■) and ethidium bromide (3.9 μM) in the presence of *E. coli* Phe-tRNA^{Phe} (1.8 μM) either in the absence (●) or in the presence of EF-Tu·GTP (4.0 μM) (▲). Curves represent best-fit analyses to the phase and modulation (not shown) data points.

from the Phe-tRNA^{Phe}-Fl^8 sample before addition of EF-Tu·GTP or after the release of tRNA from the ternary complex by the addition of excess GDP (5 mM). This approach is reasonable since the rotational parameters for tRNA^{Phe}-Fl^8 and Phe-tRNA^{Phe}-Fl^8 were essentially the same. In addition, we felt that using the same sample to determine the parameters for both free and bound Phe-tRNA^{Phe}-Fl^8 would minimize error from sample deviation. The rotational parameters reported in Table II, then, represent those values attributed to the stated species alone.

Dynamic polarization data for ethidium bromide alone in solution, bound to tRNA, and bound to tRNA in the presence of EF-Tu·GTP (Figure 4) show excellent agreement between the theoretical fits and actual data points. Rotational parameters for the various species, averaging over multiple samples, show a standard deviation of 10% or less (Table II). Lifetime results on the same samples were used in resolving the rotational components. Fluorescence contributions of the free and the tRNA-bound fluorophore were determined with the lifetime results subsequently fixed in the dynamic polarization analysis. In the samples containing EF-Tu·GTP, the rotational characteristics and fraction of unacylated, and therefore uncomplexed, tRNA^{Phe} were also fixed in the rotational analyses (cf. above). Rotational relaxation times for tRNA^{Phe} and Phe-tRNA^{Phe} were assumed to be the same, since the rotational relaxation times were nearly identical for unacylated yeast tRNA^{Phe} and for acylated *E. coli* Phe-tRNA^{Phe}.

Both global and local rotational relaxation times were resolved for the ethidium bromide bound to tRNA. Analogous to the ethidium bromide lifetime case, if the tRNA concentration and tRNA/ethidium bromide ratio were high, the secondary relaxation time decreased in amplitude (Table II). This observation suggests that the majority of the local relaxation time is due to the "secondary" ethidium bromide binding site(s). The tight ethidium binding site shows little local motion.

Discussion

Steady-state and time-resolved fluorescence measurements, such as those discussed in these studies, can provide information about both global hydrodynamic aspects of macromolecular complexes and smaller conformational alterations in the immediate vicinity of the probe. In our fluorescein–tRNA system, the fluorescein has been localized at the s^{4}U$_8$ residue of Phe-tRNA^{Phe}-Fl^8, at the juncture of the two arms of the L-shaped tRNA (Johnson et al., 1982). In the absence of EF-Tu·GTP, its lifetime is 4.29 ns, slightly longer than that of free fluorescein in alkaline solution (4.05 ns). Upon RNase digestion of tRNA^{Phe}-Fl^8 the lifetime decreases to 4.09 ns, suggesting that the radiative decay rate of the fluorescein moiety is sensitive to the details of its local environment in the intact tRNA.

Conformational changes in tRNA have been investigated by many groups where attention has focused primarily on the tRNA solution structure under varying ionic strengths, including the specific effects of magnesium ions [reviewed in Crothers and Cole (1978)]. Of particular interest here, some studies have suggested that tRNA aminoacylation causes conformational alterations in regions of the tRNA that are distant from the aminoacyl end [Potts et al. (1981) and references cited therein]. Yet we observed very little difference between the lifetime of aminoacylated (τ = 4.29 ns) or unacylated (τ = 4.27) tRNA^{Phe}-Fl^8, which indicates that significant conformational changes do not occur, upon aminoacylation, in the region of the tRNA monitored by the probe or that any conformational changes which do occur do not alter the excited-state lifetime of the probe.

Our dynamic polarization results also bear on the question of conformational alterations in tRNA that accompany aminoacylation. Potts et al. (1981) reported a measurable increase in the translational diffusion coefficient for tRNA upon aminoacylation; these results were interpreted as evidence for significant overall structural changes in the tRNA. However, our methods, which probe both the global rotational diffusion of the tRNA and the local motion of the fluorescent probe, gave no evidence for alterations in either of these parameters upon aminoacylation. Specifically, we found global rotational relaxation times of 95 and 97 ns, respectively, for tRNA^{Phe}-Fl^8 and Phe-tRNA^{Phe}-Fl^8 (Table II). Similarly, the ethidium probe did not reveal any difference between aminoacylated and unacylated tRNA (Table II).

Structural differences between unacylated and aminoacylated tRNAs have also been investigated by using spin-label probes covalently attached to s^{4}U$_8$. An initial report of aminoacylation-dependent conformational changes in tRNA (Caron et al., 1976) was later reevaluated, and the investigators concluded that the aforementioned conformational alterations did not occur (Rodriguez et al., 1980). Another group has also reported that their s^{4}U$_8$-bound spin labels detected no significant change in the overall tRNA structure upon aminoacylation (Bondarev et al., 1982). Hence, neither the spin-label probes nor the fluorescence probes used here provide any evidence for a conformational change upon aminoacylation.

Unlike the fluorescein case, ethidium bromide binding sites are noncovalent, and their positions and numbers are less well understood (Bittman, 1969; Wells & Cantor, 1977; Jones et

al., 1978; Liebman et al., 1977). Ethidium bromide, though, does have several advantages. It is more environmentally sensitive than fluorescein (and therefore more likely to be influenced by changes in its surroundings), has a longer lifetime than fluorescein (which facilitates polarization studies on large macromolecules such as the ternary complex), and binds to nucleic acids via intercalation or stacking (which results in substantially reduced local mobility compared to covalently attached probes). Although the ethidium binding sites in solution have not been unequivocally determined, crystal studies have placed the single tight binding site at the tRNA "P-10" cavity area (Liebman et al., 1977) near the same s^4U_8 residue to which the fluorescein probe is covalently attached in $tRNA^{Phe}$-Fl[8]. Spectral changes monitored with either ethidium or fluorescein will therefore result from structural changes in the same general region of the tRNA.

In contrast to the indifference of our two probes to the aminoacylation state of tRNA, each probe provides clear spectral evidence of the association of aa-tRNA with EF-Tu·GTP to form a ternary complex. For example, the association of Phe-$tRNA^{Phe}$-Fl[8] with EF-Tu·GTP to form the ternary complex did not alter the 4.3-ns lifetime of the tRNA-bound fluorescein moiety (Table I). However, a significant change in the fluorescence intensity of the Phe-$tRNA^{Phe}$-Fl[8] upon ternary complex formation has been observed and attributed to conformational changes in the tRNA molecule upon association with EF-Tu·GTP that ultimately affect the extinction coefficient of the fluorescein (Adkins et al., 1983). Our results on the lifetime invariance are consistent with this interpretation: the intensity increase upon complex formation is not due to an increase in the radiative rate constant of the probe, which suggests that the quantum yield is unaffected.

In addition, lifetime data show small differences between free Phe-$tRNA^{Phe}$ and Phe-$tRNA^{Phe}$ bound to EF-Tu·GTP in the fractional contributions of free and tRNA-bound ethidium bromide to the total fluorescence intensity. However, the extent of the observed spectral change does not correlate directly with the extent of the structural change since the intensity of bound ethidium is approximately 14-fold higher than that of free ethidium. The apparent K_d of the tight binding site, based upon lifetime data, is 6 μM for free aa-tRNA and 9 μM for aa-tRNA in the ternary complex (assuming a direct proportionality between fluorescence lifetime and quantum yield). This difference, though small and subject to uncertainties in the fractional weights, is consistent with the results of others (Adkins et al., 1983), i.e., that the formation of the ternary complex reduces the affinity of ethidium bromide for tRNA. These data suggest that the region of ethidium bromide binding on aa-tRNA undergoes structural changes that, perhaps subtly, alter the tight ethidium binding site upon association with EF-Tu·GTP.

Our dynamic polarization results indicate that the local rotations of the covalently attached fluorescein probe, ρ = 2.4 ns, remain unchanged after the ternary complex is formed (Table II), which suggests that the EF-Tu·GTP does not bind close enough to the s^4U_8 region of the aa-tRNA to interfere with the probe's rotational freedom. This assessment is in agreement with previous iodide ion quenching studies (Adkins et al., 1983) and ribonuclease digestion experiments (Jekowsky et al., 1977). In contrast, kethoxal modification data have been interpreted as indicating that the aa-tRNA D-stem and D-loop are directly protected by EF-Tu·GTP in the ternary complex (Bertram & Wagner, 1982). On the basis of the results reported here and previously, it seems more likely that tRNA sites are not directly "protected" from the kethoxal modification by EF-Tu but that EF-Tu-induced structural changes in this region of the aa-tRNA molecule interfere with the kethoxal reaction with G residues.

The global relaxation times for Phe-$tRNA^{Phe}$ of 97 ns (fluorescein) and 140 ns (ethidium bromide) are longer than the 83-ns value calculated for a sphere with the same volume as the hydrated tRNA molecule (Table II). This result demonstrates the asymmetric nature of the tRNA molecule in solution. Both measured values are consistent with relaxation times previously reported in the literature, which have ranged from 90 to 145 ns, after correcting to 5 °C for temperature and viscosity (Tao et al., 1970; Thomas et al., 1984; Ferguson & Yang, 1986). Although both fluorescein and ethidium probes appear to be located in the same region of the tRNA [see Adkins et al. (1983)], their global rotational relaxation times differ considerably. This difference probably results from the particular orientation of each fluorophore's absorption and emission dipoles with respect to the macromolecular rotational axes of transfer RNA. The observed global rotational relaxation times are thus an average that reflects the weighted contributions of the rotation about each macromolecular axis (Beechem et al., 1986). The average of the fluorescein- and ethidium-detected rotational rates corresponds to that of a prolate ellipsoid with an axial ratio of 3:1. Our results therefore agree with estimates made by others (Tao et al., 1970) and with the reported crystal structure (Sussman & Kim, 1976).

Interestingly, information on the size and shape of EF-Tu indicates that it too is quite asymmetric, and it models as an oblate ellipsoid with an axial ratio of 4:1 (Sjöberg and Elias, 1978). This finding is consistent with the crystallography work done on trypsinized EF-Tu·GDP (Morikawa et al., 1978; Jurnak, 1985; LaCour et al., 1985). Results from this laboratory using fluorescence methodologies have also shown EF-Tu·GDP to be asymmetric (Jameson et al., 1987; Eccleston et al., 1987).

Both fluorescein and ethidium report a large increase in global relaxation time for the aa-tRNA upon ternary complex formation (Table II). As with free Phe-$tRNA^{Phe}$(-Fl[8]), the observed value differs for each probe, a result that by itself shows the asymmetric nature of the ternary complex and the different orientation of the two fluorophores within the ternary complex. The ratio of the observed relaxation time for the ternary complex relative to that calculated for a sphere of equal volume was 1.4 and 1.1 for ethidium bromide and fluorescein, respectively. In contrast, the equivalent ratios for Phe-$tRNA^{Phe}$ were 1.7 and 1.2 for ethidium bromide and fluorescein, respectively, slightly larger than those found for the ternary complex and hence indicative of a more asymmetric hydrodynamic structure. Thus, our results suggest that the ternary complex is less asymmetric than either tRNA or EF-Tu.

If, for example, these data were modeled by assuming prolate ellipsoids, then the axial ratios of these ellipsoids for Phe-$tRNA^{Phe}$ and ternary complex (using the ethidium bromide results) would be 4.2:1 and 2.6:1, respectively. Consequently, it is unlikely that Phe-$tRNA^{Phe}$ binds to EF-Tu end to end, since one would expect a molecular arrangement of this type to increase the observed global relaxation time. Instead, our results are more consistent with a macromolecular arrangement that is largely side by side, since this orientation would reduce the observed asymmetry. In such a complex, the EF-Tu·GTP would bind to the side of the aa-tRNA on which the extra loop is exposed (Wikman et al., 1982; Kao et al., 1983) and not on the side that exposes the D-loop and

s^4U_8 region (Adkins et al., 1983). Our data are therefore more compatible with the results of the small-angle neutron scattering studies (Antonsson et al., 1986) that suggest a compact ternary complex rather than with the small-angle X-ray scattering data (Österberg et al., 1981) that suggest a more extended complex.

In conclusion, we have demonstrated that time-resolved fluorescence methods, in particular the multifrequency phase and modulation technique, may be utilized to gain information on structural, hydrodynamic, and dynamic aspects of the ternary complex. Ultimately, this information, combined with more extensive studies using additional probes and energy-transfer methods, should afford us more insight into the overall topography of the ternary complex, specifically the relative dispositions of the macromolecular partners.

ACKNOWLEDGMENTS

We are grateful to Vickey Thomas for technical assistance and to Jo Hicks for word processing. We also would like to thank Dr. Clive Slaughter and Carolyn Moomaw for the quantitative amino acid analysis.

REFERENCES

Abrahamson, J. K., Laue, T. M., Miller, D. L., & Johnson, A. E. (1985) *Biochemistry 24*, 692–700.

Adkins, H. J., Miller, D. L., & Johnson, A. E. (1983) *Biochemistry 22*, 1208–1217.

Alcala, J. R., Gratton, E., & Prendergast, F. G. (1987) *Biophys. J. 51*, 587–596.

Antonsson, B., Leberman, R., Zaccai, G., & Jacrat, B. (1986) *Biochemistry 25*, 3655–3659.

Arai, K.-I., Kawakita, M., Kaziro, Y., Kondo, T., & Ui, N. (1973) *J. Biochem. (Tokyo) 73*, 1095–1105.

Arai, K., Clark, B. F. C., Duffy, L., Jones, M. D., Kaziro, Y., Laursen, R. A., L'Italien, J., Miller, D. L., Nagarkatti, S., Nakamura, S., Nielsen, K. M., Petersen, T. E., Takahashi, K., & Wade, M. (1980) *Proc. Natl. Acad. Sci. U.S.A. 77*, 1326–1330.

Barrell, B. G., & Sanger, F. (1969) *FEBS Lett. 3*, 275–278.

Beechem, J. M., Knutson, J. R., & Brand, L. (1986) *Biochem. Soc. Trans. 14*, 832–835.

Bertram, S., & Wagner, R. (1982) *Biochem. Int. 4*, 117–126.

Bittman, R. (1969) *J. Mol. Biol. 46*, 251–268.

Bock, R. M., Ling, N.-S., Morell, S. A., & Lipton, S. H. (1956) *Arch. Biochem. Biophys. 62*, 253–264.

Bondarev, G. N., Isaev-Ivanov, V. V., Isaeva-Ivanova, L. S., Kirillov, S. V., Kleiner, A. R., Lepekhin, A. F., Odinzov, V. B., & Fomichev, V. N. (1982) *Nucleic Acids Res. 10*, 1113–1126.

Boutorin, A. S., Clark, B. F. C., Ebel, J. P., Kruse, T. A., Petersen, H. U., Remy, P., & Vassilenko, S. (1981) *J. Mol. Biol. 152*, 593–608.

Caron, M., Brisson, N., & Dugas, H. (1976) *J. Biol. Chem. 251*, 1529–1530.

Claesens, F., & Rigler, R. (1986) *Eur. Biophys. J. 13*, 331–342.

Cohn, E. J., & Edsall, J. T. (1943) *Proteins, Amino Acids and Peptides as Ions and Dipolar Ions*, Reinhold Publishing Co., New York, NY.

Crothers, D. M., & Cole, P. E. (1978) in *Transfer RNA* (Altman, S., Ed.) pp 196–247, MIT Press, Cambridge, MA.

Duffy, L. K., Gerber, L., Johnson, A. E., & Miller, D. L. (1981) *Biochemistry 20*, 4663–4666.

Eccleston, J. F., Gratton, E., & Jameson, D. M. (1987) *Biochemistry 26*, 3902–3907.

Edelhoch, H. (1967) *Biochemistry 6*, 1948–1954.

Ferguson, B. Q., & Yang, D. C. H. (1986) *Biochemistry 25*, 5298–5304.

Gratton, E., & Limkeman, M. (1983) *Biophys. J. 44*, 315–324.

Gratton, E., Jameson, D. M., & Hall, R. D. (1984) *Annu. Rev. Biophys. Bioeng. 13*, 105–124.

Holbrook, S. R., Sussman, J. L., Warrant, R. W., & Kim, S.-H. (1978) *J. Mol. Biol. 123*, 631–660.

Hudson, B., & Jacobs, R. (1975) *Biopolymers 14*, 1309–1312.

Jameson, D. M., Gratton, E., & Hall, R. D. (1984) *Appl. Spectrosc. Rev. 20*, 55–106.

Jameson, D. M., Gratton, E., & Eccleston, J. F. (1987) *Biochemistry 26*, 3894–3901.

Jekowsky, E., Schimmel, P. R., & Miller, D. L. (1977) *J. Mol. Biol. 114*, 451–458.

Johnson, A. E., Miller, D. L., & Cantor, C. R. (1978) *Proc. Natl. Acad. Sci. U.S.A. 75*, 3075–3079.

Johnson, A. E., Adkins, H. J., Matthews, E. A., & Cantor, C. R. (1982) *J. Mol. Biol. 156*, 113–140.

Johnson, A. E., Janiak, F., Dell, V. A., & Abrahamson, J. K. (1986) in *Structure, Function, and Genetics of Ribosomes* (Hardesty, B., & Kramer, G., Eds.) pp 541–555, Springer-Verlag, New York.

Jones, C. R., Bolton, P. H., & Kearns, D. R. (1978) *Biochemistry 17*, 601–607.

Jurnak, F. (1985) *Science 230*, 32–36.

Kao, T.-H., Miller, D. L., Abo, M., & Ofengand, J. (1983) *J. Mol. Biol. 166*, 383–405.

Kim, S.-H., & Rich, A. (1968) *Science 162*, 1381–1384.

Kim, S.-H., Suddath, F. L., Quigley, G. J., McPherson, A., Sussman, J. L., Wang, A. H. J., Seeman, N. C., & Rich, A. (1974) *Science 185*, 435–440.

LaCour, T. F. M., Nyborg, J., Thirup, S., & Clark, B. F. C. (1985) *EMBO J. 4*, 2385–2388.

Ladner, J. E., Finch, J. T., Klug, A., & Clark, B. F. C. (1972) *J. Mol. Biol. 72*, 99–101.

Laursen, R. A., L'Italien, J. J., Nagarkatti, S., & Miller, D. L. (1981) *J. Biol. Chem. 256*, 8102–8109.

Leberman, R., Antonsson, B., Giovanelli, R., Guariguata, R., Schumann, R., & Wittinghofer, A. (1980) *Anal. Biochem. 104*, 29–36.

Liebman, M., Rubin, J., & Sundaralingam, M. (1977) *Proc. Natl. Acad. Sci. U.S.A. 74*, 4821–4825.

McMeekin, T. L., Groves, M. L., & Hipp, N. J. (1949) *J. Am. Chem. Soc. 71*, 3298–3300.

Miller, D. L., & Weissbach, H. (1974) *Methods Enzymol. 30*, 219–232.

Miller, D. L., & Weissbach, H. (1977a) in *Molecular Mechanisms of Protein Biosynthesis* (Weissbach, H., & Pestka, S., Eds.) pp 323–373, Academic Press, New York.

Miller, D. L., & Weissbach, H. (1977b) in *Nucleic Acid–Protein Recognition* (Vogel, H. J., Ed.) pp 409–440, Academic Press, New York.

Morikawa, K., LaCour, T. F. M., Nyborg, J., Rasmussen, K. M., Miller, D. L., & Clark, B. F. C. (1978) *J. Mol. Biol. 125*, 325–338.

Österberg, R., Sjöberg, B., Ligaarden, R., & Elias, P. (1981) *Eur. J. Biochem. 117*, 155–159.

Potts, R. O., Ford, N. C., Jr., & Fournier, M. J. (1981) *Biochemistry 20*, 1653–1659.

Rigler, R., & Wintermeyer, W. (1983) *Annu. Rev. Biophys. Bioeng. 12*, 475–505.

Rodriguez, A., Tougas, G., Brisson, N., & Dugas, H. (1980) *J. Biol. Chem. 255*, 8116–8120.

Schmidt, P. G., Sierzputowska-Gracz, H., & Agris, P. F. (1987) *Biochemistry 26*, 8529–8534.

Sigler, P. B. (1975) *Annu. Rev. Biophys. Bioeng. 4*, 477–527.
Sjöberg, B., & Elias, P. (1978) *Biochim. Biophys. Acta 519*, 507–512.
Sussman, J. L., & Kim, S.-H. (1976) *Science 192*, 853–858.
Sussman, J. L., Holbrook, S. R., Warrant, R. W., Church, G. M., & Kim, S.-H. (1978) *J. Mol. Biol. 123*, 607–630.
Tao, T., Nelson, J. H., & Cantor, C. R. (1970) *Biochemistry 9*, 3514–3524.
Thomas, J. C., Schurr, J. M., & Hare, D. R. (1984) *Biochemistry 23*, 5407–5413.
Uziel, M., & Gassen, H. G. (1969) *Biochemistry 8*, 1643–1655.
van Noort, J. M., Kraal, B., Bosch, L., LaCour, T. F. M., Nyborg, J., & Clark, B. F. C. (1984) *Proc. Natl. Acad. Sci. U.S.A. 81*, 3969–3972.
Weber, G. (1977) *J. Chem. Phys. 66*, 4081–4091.
Wells, B. D., & Cantor, C. R. (1977) *Nucleic Acids Res. 4*, 1667–1680.
Wikman, F. P., Siboska, G. E., Petersen, H. U., & Clark, B. F. C. (1982) *EMBO J. 1*, 1095–1100.

High-Level Expression, Purification, and Characterization of Recombinant Human Tumor Necrosis Factor Synthesized in the Methylotrophic Yeast *Pichia pastoris*

K. Sreekrishna,* Lynn Nelles, Rica Potenz,‡ John Cruze,§ Paul Mazzaferro,‖ Wayne Fish, Motohiro Fuke,⊥ Kathy Holden,‖ Doris Phelps, Phyllis Wood, and Kathryn Parker

Phillips Petroleum Company, Bartlesville, Oklahoma 74004

Received August 8, 1988; Revised Manuscript Received November 29, 1988

ABSTRACT: Human tumor necrosis factor (TNF) α/cachectin was expressed in the methylotrophic yeast *Pichia pastoris* at high levels (>30% of the soluble protein) by placing the TNF cDNA under the control of regulatory sequences derived from the alcohol oxidase gene. Batch fermentor cultures at cell densities of 50 and 85 g dry cell weight/L contained approximately 6×10^{10} and 10^{11} units/L TNF bioactivity (6 and 10 g/L TNF), respectively. TNF productivity of 0.108 g L^{-1} h^{-1} was obtained in the continuous mode on glycerol- and methanol-mixed feed at 25 g dry cell weight/L cell density. TNF contained in the yeast cell lysate was soluble, displayed full cytotoxic activity, and was recognized by antibodies prepared against TNF derived from *Escherichia coli*. TNF was purified to >95% purity with >75% recovery by using three sequential chromatographic steps with a coordinated effluent–affluent buffer scheme which allowed one eluate to also serve as the loading buffer for the succeeding column. The amino acid composition, NH_2-terminal amino acid sequence, isoelectric point, and minimal molecular weight determined for TNF corroborated those properties predicted from the nucleotide sequence. Sedimentation data indicated that TNF in the native form is a compact trimer held by noncovalent interactions. Circular dichroic spectra of TNF resemble those of proteins with high β structure. TNF exhibited cachectic activity on mouse 3T3-L1 cells at about the same equivalence as the cytotoxic activity toward mouse L929 cells. In the criteria examined, TNF derived from *P. pastoris* closely resembles TNF derived from recombinant *E. coli* and human HL-60 cells.

Tumor necrosis factor (TNF)[1] is an antitumor protein found in the sera of animals that have been primed with microbial materials such as BCG (Bacillus Calmette Guerin), *Corynebacterium parvum*, or zymosan and subsequently treated with lipopolysaccharides (LPS, a major constituent of the cell wall of Gram-negative bacteria also known as endotoxin or bacterial pyrogen) (Old, 1985). The cellular origin of TNF is macrophages (monocytes) (Carswell et al., 1975; Hoffmann et al., 1978; Mannel et al., 1980; Satomi et al., 1981). TNF causes hemorrhagic necrosis and regression of certain tumors transplanted in mice (Carswell et al., 1975; Kull & Cuatrecasas, 1981). TNF shows cytotoxic activity against certain tumor cell lines (Carswell et al., 1975; Ostrove & Gifford, 1979; Haranaka & Satomi, 1981). TNF is identical with cachectin, one of the principal mediators of the lethal effect of LPS (Beutler et al., 1985). Cachectin inhibits the biosynthesis of lipoprotein lipase and other enzymes required for de novo triglyceride synthesis in adipocytes (Pekala et al., 1983). Cachectin also suppresses the expression of mRNAs produced specifically by mature adipose tissue cells (Torti et al., 1985) and prevents the morphological differentiation of adipocytes in vitro.

The human TNF gene has been cloned (Pennica et al., 1984; Shirai et al., 1985; Wang et al., 1985; Shomura et al., 1985; Maremenout et al., 1985; Yamada et al., 1985; Berent et al., 1986) and found to be present as one copy per haploid genome on chromosome 6 (Nedwin et al., 1985; Spies et al., 1986).

* Address correspondence to this author.
‡ Present address: Abbott Laboratories, Chicago, IL 60064.
§ Present address: GMT Inc., Ochelata, OK 74501.
‖ Present address: Bissendorf Biosciences Inc., Richardson, TX 75083.
⊥ Present address: JA Bio Inc., Tulsa, OK 74137.

[1] Abbreviations: BCG, Bacillus Calmette Guerin; CD, circular dichroism; CPG, controlled pore glass; DO, dissolved oxygen; ELISA, enzyme-linked immunosorbent assay; GdmCl, guanidinium chloride; HPLC, high-performance liquid chromatography; LPS, lipopolysaccharides; M_r, molecular weight; PMSF, phenylmethanesulfonyl fluoride; PTC, phenylthiocarbamyl; SDS, sodium dodecyl sulfate; SDS–PAGE, sodium dodecyl sulfate–polyacrylamide gel electrophoresis; TEOA, triethanolamine; TNF, tumor necrosis factor; UV, ultraviolet.

0006-2960/89/0428-4117$01.50/0